

RESEARCH ARTICLE

10.1002/2017JG003775

Key Points:

- Multiple ecosystem shifts were observed within the surface 1 m of blue carbon sediments
- Preservation of inputs from prior ecosystem formation can make large contributions to contemporary carbon stocks
- Heterogeneity of historical influence needs to be accounted for in regional assessments of carbon storage

Supporting Information:

- Supporting Information S1

Correspondence to:

J. J. Kelleway,
jeffrey.kelleway@mq.edu.au

Citation:

Kelleway, J. J., N. Saintilan, P. I. Macreadie, J. A. Baldock, H. Heijnis, A. Zawadzki, P. Gadd, G. Jacobsen, and P. J. Ralph (2017), Geochemical analyses reveal the importance of environmental history for blue carbon sequestration, *J. Geophys. Res. Biogeosci.*, 122, 1789–1805, doi:10.1002/2017JG003775.



Received 18 JAN 2017

Accepted 23 JUN 2017

Accepted article online 30 JUN 2017

Published online 21 JUL 2017

Geochemical analyses reveal the importance of environmental history for blue carbon sequestration

J. J. Kelleway^{1,2,3} , N. Saintilan², P. I. Macreadie⁴, J. A. Baldock⁵, H. Heijnis⁶, A. Zawadzki⁶, P. Gadd⁶, G. Jacobsen⁶ , and P. J. Ralph¹
¹Climate Change Cluster, University of Technology Sydney, Ultimo, New South Wales, Australia, ²Department of Environmental Sciences, Macquarie University, Sydney, New South Wales, Australia, ³Now at Department of Environmental Sciences, Macquarie University, Sydney, New South Wales, Australia, ⁴School of Life and Environmental Sciences, Centre for Integrative Ecology, Deakin University, Burwood, Victoria, Australia, ⁵CSIRO Agriculture and Food, Glen Osmond, South Australia, Australia, ⁶Australian Nuclear Science and Technology Organisation, Lucas Heights, New South Wales, Australia

Abstract Coastal habitats including saltmarshes and mangrove forests can accumulate and store significant blue carbon stocks, which may persist for millennia. Despite this implied stability, the distribution and structure of intertidal-supratidal wetlands are known to respond to changes imposed by geomorphic evolution, climatic, sea level, and anthropogenic influences. In this study, we reconstruct environmental histories and biogeochemical conditions in four wetlands of similar contemporary vegetation in SE Australia. The objective is to assess the importance of historic factors to contemporary organic carbon (C) stocks and accumulation rates. Results from the four cores—two collected from marine-influenced saltmarshes (Wapengo marine site (WAP-M) and Port Stephens marine site (POR-M)) and two from fluvial influenced saltmarshes (Wapengo fluvial site (WAP-F) and Port Stephens fluvial site (POR-F))—highlight different environmental histories and preservation conditions. High C stocks are associated with the presence of a mangrove phase below the contemporary saltmarsh sediments in the POR-M and POR-F cores. ¹³C nuclear magnetic resonance analyses show this historic mangrove root C to be remarkably stable in its molecular composition despite its age, consistent with its position in deep sediments. WAP-M and WAP-F cores did not contain mangrove root C; however, significant preservation of char C (up to 46% of C in some depths) in WAP-F reveals the importance of historic catchment processes to this site. Together, these results highlight the importance of integrating historic ecosystem and catchment factors into attempts to upscale C accounting to broader spatial scales.

1. Introduction

1.1. Organic Carbon in Coastal Ecosystems

Coastal vegetated habitats (saltmarshes, mangrove forests, and seagrass beds) provide an important ecosystem service through the capture and long-term storage of organic carbon (C). This capacity to sequester “blue carbon” is dependent upon three broad ecosystem factors: (1) high productivity in converting CO₂ into plant biomass C [Alongi, 2002; Nixon, 1980], (2) effective trapping of particulate organic C originating from within the ecosystem (autochthonous C) and/or from external sources (allochthonous C) [Kennedy *et al.*, 2010], and (3) biogeochemical conditions within sediments which slow the decay of organic material [Fourqurean *et al.*, 2012; Kristensen *et al.*, 2008; McLeod *et al.*, 2011]. In concert, these factors may allow C-rich sediments and biomass to continue to accrete over centuries and millennia [Lo Iacono *et al.*, 2008; McKee *et al.*, 2007]. Consequently, coastal vegetated habitats generally contain higher belowground stocks of C over a given depth and accumulate C in surface sediments faster than most terrestrial habitats [Fourqurean *et al.*, 2012; McLeod *et al.*, 2011].

Much of the blue carbon accumulated over time is produced belowground by roots and rhizomes [Pendleton *et al.*, 2012], though contributions from other sources may be significant. A global assessment of seagrass C isotope values (δ¹³C), for example, revealed that on average ~50% of all C in surface seagrass sediments derives from nonseagrass sources [Kennedy *et al.*, 2010]. Contributions of autochthonous versus allochthonous inputs may vary substantially, however, among the different depositional settings in which blue carbon ecosystems are found [Kelleway *et al.*, 2016a; Zhou *et al.*, 2006]. Such variability may have implications for long-term C storage because the molecular composition (i.e., recalcitrance) of C inputs is

considered a key driver of decay rates [Enríquez *et al.*, 1993], including in blue carbon ecosystems [Kristensen, 1994]. For example, it was recently demonstrated that organic matter stability decreases among marine macrophytes in the order mangrove > saltmarsh plants > seagrass > macroalgae, consistent with variations in molecular composition among taxa [Trevathan-Tackett *et al.*, 2015]. Terrestrial inputs to marine sediments, including lignin-rich plant materials and char transported after catchment fires, have also been shown to have high resistance to decomposition [Burdige, 2007, and references therein; Derenne and Largeau, 2001].

Whatever the C source, the capacity of coastal wetlands to store carbon over the long-term is dependent upon the balance between inputs and their decay rate [Kirwan *et al.*, 2013]. Due to low oxygen diffusion in water-saturated sediments, microbial decomposition of C in blue carbon sediments occurs mainly through anaerobic metabolic pathways [Howes *et al.*, 1984; King, 1983; Lord and Church, 1983]. The decomposition of organic matter also increases the diversity of biomolecules in soils and sediments as microbes transform source materials, synthesize additional biochemicals for their own growth, and excrete products of metabolic activity [Baldock *et al.*, 2013; Grandy and Neff, 2008].

1.2. Understanding Blue Carbon Variability

Considerable research effort over the past decade has greatly improved blue carbon sequestration estimates over local, regional, and global scales. Spatial variability of C stocks and C accumulation rates has been assessed in terms of contemporary expressions of vegetation composition and structure [Chen *et al.*, 2015; Kelleway *et al.*, 2016b; Ricart *et al.*, 2015] as well as geomorphic and sedimentary properties [e.g., Adame *et al.*, 2010; Donato *et al.*, 2011; Macreadie *et al.*, 2017; Serrano *et al.*, 2016b]. Such studies based on contemporary ecosystem character improve our understanding of C stocks and surface processes and have applicability in upscaling estimates to broader spatial scales [e.g., Duarte *et al.*, 2013; Pendleton *et al.*, 2012]. They often fail, however, to capture the variability driven by subsurface processes such as deep root growth [Lovelock *et al.*, 2013] and the preservation (or decay) of deep organic matter which may have accumulated hundreds or thousands of years earlier [Lo Iacono *et al.*, 2008; McKee *et al.*, 2007]. Improved knowledge of surface and subsurface blue carbon processes will become increasingly important as coastal wetlands respond to changes imposed by geomorphic, climatic, sea level, and anthropogenic influences [Kirwan and Megonigal, 2013; Swales *et al.*, 2015; Woodroffe *et al.*, 1985].

In southeastern (SE) Australia, the dynamic nature of blue carbon ecosystems has been revealed through analyses of sediment cores collected throughout the region. Mangrove roots have been found preserved beneath contemporary saltmarsh surface in multiple locations [Saintilan and Hashimoto, 1999; Saintilan and Wilton, 2001]; however, this phenomenon is not universal [Kelleway *et al.*, 2016a; Mitchell and Adam, 1989]. It is possible that site-specific differences in the input and preservation of roots explain some of the of spatial variability in subsurface C density of saltmarsh sediments that is not readily explained by contemporary (surface) vegetation structure or sedimentary properties [Kelleway *et al.*, 2016a].

The current study aims to reconstruct environmental histories and biogeochemical conditions in four wetlands of similar contemporary vegetation in SE Australia. It will do this by combining high-resolution chemical profiles with discrete sampling of parameters informative of the wetland's developmental stage, organic matter stocks and sources, and preservation or processing of C. The objective is to assess the importance of historic C input and preservation to contemporary blue carbon stocks and C accumulation rates.

2. Materials and Methods

2.1. Study Setting

In SE Australia, saltmarsh and mangrove ecosystems are restricted to estuaries and marine embayments where hydrodynamic energy is sufficiently reduced to allow colonization and survival of plants [West *et al.*, 1985]. Within these estuaries and embayments the most recent phase of estuarine sedimentation was initiated about 7000–8000 years ago [Roy, 1984; Roy and Thom, 1981] though rates of infilling of individual valleys have varied spatially since then [Roy *et al.*, 2001]. The four sedimentary environments in SE Australian estuaries (marine tidal delta, central mud basin, fluvial delta, and riverine channel) have characteristic water quality and nutrient cycling/primary productivity signatures [Roy *et al.*, 2001]. Of these, the marine

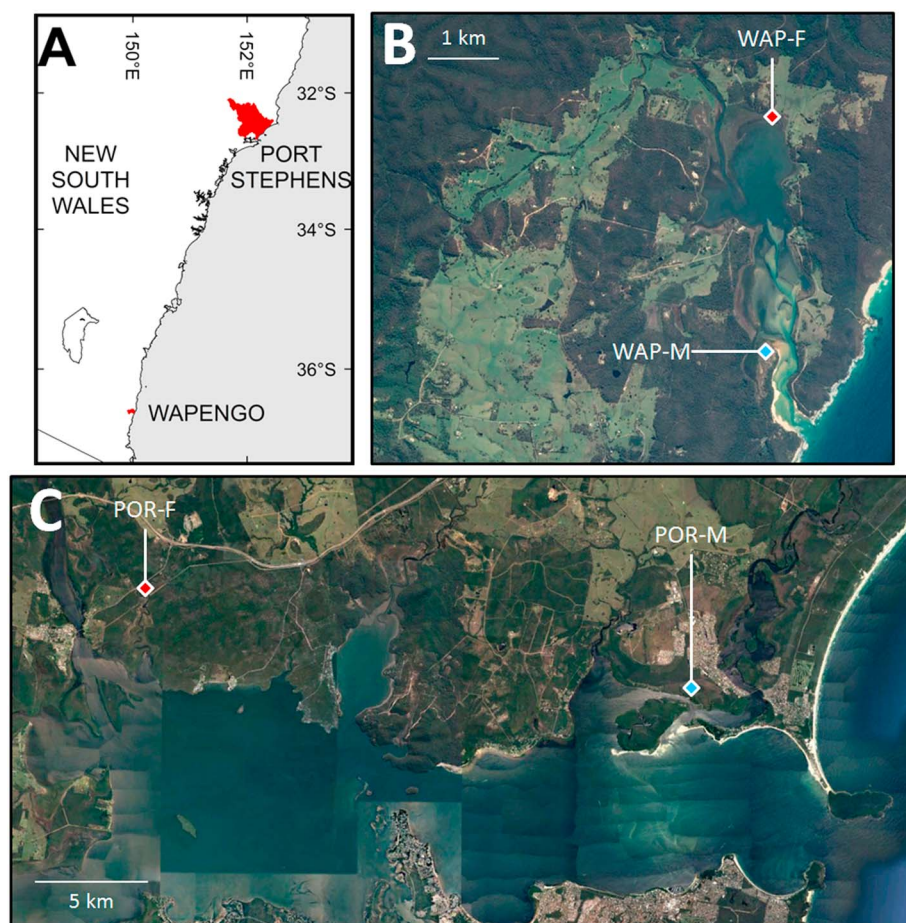


Figure 1. (a) Location of study estuaries along the New South Wales coast of SE Australia, (b) location of WAP-M and WAP-F in Wapengo Lagoon, and (c) location of POR-M and POR-F in the Port Stephens estuary.

tidal delta and fluvial delta represent depositional environments with distinctly different sedimentary sources, and as such these two zones will be a focus of this study.

SE Australian saltmarsh communities generally have low floral species richness, often being dominated by just one or two species [Adam *et al.*, 1988]. There are broad zonation patterns coinciding with surface elevation, whereby the majority of lower to midelevation saltmarsh is considered a single association dominated by the chenopod *Sarcocornia quinqueflora* and grass *Sporobolus virginicus* [Zedler *et al.*, 1995]. Data previously collected within the study region show that aboveground biomass of this association is low (*S. quinqueflora* mean = 320 g m^{-2} ; *S. virginicus* mean = 350 g m^{-2}) relative to other saltmarsh types [Clarke and Jacoby, 1994]. Throughout mainland Australia, saltmarshes are generally bordered downslope by mangroves (the species *Avicennia marina* is dominant throughout the region) and supratidal forest or shrub communities to the higher, landward side.

The estuaries of Wapengo Lagoon and Port Stephens (Figure 1) were chosen for this study based on their dissimilarity in geomorphic type and stage of infilling. Within each estuary a saltmarsh near the estuary mouth was chosen as a “marine” influenced site, while a saltmarsh further up the estuary was chosen as a “fluvial” influenced site. For each site, a single sediment core was selected randomly from among five replicate cores from the midmarsh (i.e., the *Sarcocornia-Sporobolus* association) collected as part of a previous study [Kelleway *et al.*, 2016a].

2.2. Wapengo Lagoon

Wapengo Lagoon is a small, semimature barrier estuary (water area = 3.2 km^2 ; catchment area = 73 km^2) with an estimated tidal range of 0.45 m and average estuary depth of just 1.29 m below mean high tide [Roy *et al.*,

2001; Roper *et al.*, 2011]. The contemporary extent of saltmarsh, mangrove forest, and seagrass beds in Wapengo Lagoon is 0.51, 0.56, and 0.42 km², respectively [Creese *et al.*, 2009]. While the upper Wapengo catchment is vegetated by native forests, much of the lower catchment has been cleared. Clearing likely occurred from the 1840s onward, when grazing and then timber milling operations expanded through the region [NSW National Parks and Wildlife Service, 2011]. In total, approximately 16% of the catchment has now been cleared [Roper *et al.*, 2011].

The Wapengo marine site (referred to hereafter as WAP-M) is located in the lower estuary, within Mimosa Rocks National Park. The succulent species *S. quinqueflora* (C3 photosynthetic pathway) is the dominant saltmarsh plant. The mangrove *Avicennia marina* (C3) occupies large areas of the site, but its distribution is scattered and restricted to dwarf shrubs within the vicinity of the coring location (~15 m away).

The Wapengo fluvial site (WAP-F) is located on a fluvial delta formed by the confluence of the main river into the estuary and an unnamed creek with a smaller subcatchment. The lower parts of this subcatchment, including the areas immediately upslope of WAP-F, have been extensively cleared for agriculture with small farm dams installed across drainage lines, sometime after the 1840s. The core was collected approximately 25 m from the small creek within a band of saltmarsh dominated by *S. quinqueflora*. Dwarf shrubs of *A. marina* are distributed across the fluvial delta, mostly in combination with the succulent saltmarsh shrub *Tecticornia arbuscular*, but neither occurred within 10 m of the coring location.

2.3. Port Stephens

Port Stephens is a tide-dominated, drowned valley estuary in the “youthful” stage of its geomorphic evolution [Roy *et al.*, 2001]. The main estuary has an area of 126 km² and catchment area of 4950 km² [Roy *et al.*, 2001]. In addition, two smaller estuaries—the Karuah River (3.9 km²) and Myall River (7.5 km²)—also feed into Port Stephens. Tidal range within the estuary mouth has been estimated as 1.01 m [Roper *et al.*, 2011] but is amplified up the estuary toward the Karuah River [Roy and Boyd, 1996]. The contemporary extent of saltmarsh, mangrove forest, and seagrass beds in Port Stephens is 10.63, 19.04, and 14.39 km², respectively [Creese *et al.*, 2009].

Port Stephens has a large flood-tide delta comprising shallow sand banks intersected by active tidal channels. The Port Stephens marine site (POR-M) is located in the intertidal-supratidal zone adjacent to this delta and comprises Pleistocene barrier sands overlaid by Holocene tidal delta sands [Roy and Boyd, 1996]. The sediment core was collected >100 m from the nearest open water in a meadow dominated by the C4 grass *S. virginicus*, but containing occasional *A. marina* mangrove trees in low-lying depressions. The nearest mangrove was situated approximately 25 m from the core.

A fluvial site (POR-F) was chosen within Yalimbah Creek, a tide-dominated creek which drains into the north-western corner of Port Stephens. Yalimbah Creek consists of a small tidal (mostly unvegetated) channel bordered by muddy, vegetated intertidal, and supratidal flats, and meandering through a narrow valley incised in Permo-Carboniferous bedrock [Roy and Matthei, 1996]. Yalimbah Creek has a small catchment of approximately 14.5 km² (of which ~2.2 km² is intertidal), while the spring tidal range has been measured at 1.4 m [Davies, 2011]. This small catchment remains largely forested, though a small quarry at the top of the catchment commenced operation in 2000. The POR-F sediment core was collected with an area of *S. virginicus* saltmarsh located approximately 10 m from the edge of the main channel of Yalimbah Creek (i.e., a section of creek without mangrove frontage) and 10 m from the nearest mangrove (*A. marina*).

2.4. Field Collection and Measurement

At each site, a single sediment core of 50 mm diameter and approximately 1 m depth was randomly chosen from among five extracted from the *Sarcocornia-Sporobolus* midmarsh association for a previous study. Details of coring methods and data from the other four cores collected at each site are reported in Kelleway *et al.* [2016a]. Mean carbon stocks inclusive of all five *Sarcocornia-Sporobolus* cores, plus four cores collected from upper marsh rush communities, are reported in Table 1.

2.5. ITRAX

High-resolution logging of each core was undertaken using an ITRAX Core Scanner [Croudace *et al.*, 2006] to (1) inform the reconstruction of paleo-environments and determine provenance of sediments within each site and (2) identify distinct regions of interest (ROIs) within each core from which to subsample for

Table 1. Bulk Sediment and Carbon Accumulation Rates for Surface Sediments and C Store for Entire Core Profiles for Each of the Four Study Sites^a

Site	Depth Range (cm)	Surface Accumulation Rates			C Store (0–100 cm)	
		Bulk Sediment		C	This Core	Site Mean ^b
		(mm yr ^{−1})	(Mg ha ^{−1} yr ^{−1})	(Mg C ha ^{−1} yr ^{−1})	(Mg C ha ^{−1})	(Mg C ha ^{−1})
WAP-M	0–8	2	34.6 ± 1.6	0.8 ± 0.0	37.9	63.3 ± 12.9
	8–16	1	23.9 ± 2.2	0.1 ± 0.0		
WAP-F	0–11	1	5.8 ± 0.5	0.8 ± 0.1	176.0	193.1 ± 11.4
POR-M	0–6	1	7.0 ± 1.0	0.3 ± 0.0	156.0	164.0 ± 10.3
POR-F	0–16	2	18.7 ± 1.7	0.8 ± 0.1	204.5	166.2 ± 9.5

^aAccumulation rates are based upon CIC (constant initial concentration) model of ²¹⁰Pb dating profiles, except WAP-M which is based upon a CRS model due to differing ²¹⁰Pb activities above and below 8 cm.

^bValues derived by combining this core with replicate values reported in Kelleway *et al.* [2016a]. *N* = 9.

specific analyses (¹³C nuclear magnetic resonance (NMR) and particle size analysis). Each core was scanned using a molybdenum tube set at 30 kV and 55 mA, with a dwell time of 10 s and step size of 1 mm. Six elemental ratios and related measures were selected for use as environmental proxies on the basis of their suitability in marine or estuarine sediments. In two of these ratios Ti was used as a divisor because of its stability and terrigenous provenance [Rothwell and Croudace, 2015].

The incoherent/coherent scattering ratio (inc/coh) was used as a qualitative indicator of organic matter content, with higher values of this ratio indicating increased organic content [Burnett *et al.*, 2011]. Ca/Ti was used to indicate Ca-rich marine sediment provenance (high Ca/Ti) or high terrigenous sediment delivery relative to Ca-rich marine sources (low Ca/Ti) [Rothwell and Croudace, 2015]. Si/Ti was used as a proxy for siliceous productivity, with biogenic Si derived from siliceous microfossils including diatoms [Agnihotri *et al.*, 2008]. In recent sediment samples, magnetic susceptibility (κ) is a measure of the amount of the mineral magnetite (or its oxidized derivative hematite) present by unit volume. Therefore, peaks in magnetic susceptibility may be an indicator of mineralogic inputs (mainly terrigenous soils); however, human-introduced magnetic materials and biogenic sources (including bacterially generated ferrimagnetic material) can also produce magnetic anomalies. Fe/ κ is a sensitive proxy for magnetite diagenesis, with reductive diagenesis of Fe resulting in a significant magnetic susceptibility loss by the transformation of ferrimagnetic iron minerals to paramagnetic iron compounds (i.e., indicated by peaks in Fe/ κ) [Hofmann *et al.*, 2005; Rothwell and Croudace, 2015; van der Land *et al.*, 2011]. Finally, Zr/Rb was used as a grain-size proxy as Zr resides mainly in coarser grains and Rb in clays [Rothwell and Croudace, 2015].

2.6. Radiometric Dating

Lead-210 (²¹⁰Pb) dating of surface sediments was undertaken to generate age profiles among surface sediments [Appleby and Oldfield, 1978] and to allow the calculation of both bulk sediment and C accumulation rates. For each core, six depth intervals (0–1, 2.5–3.5, 5–6, 7.5–8.5, 10–11, and 15–16 cm) were selected for preliminary analysis. Additional “fill-in” samples were analyzed as necessarily to improve the reliability of the age models. Samples were dried, measured for bulk density, and then processed to determine polonium-210 (²¹⁰Po) and radium-226 (²²⁶Ra) activities by alpha spectrometry [Atahan *et al.*, 2015]. Unsupported ²¹⁰Pb activities were estimated as the difference between total ²¹⁰Pb activity (measured from ²¹⁰Po) and supported ²¹⁰Pb activity (measured from ²²⁶Ra) [Appleby and Oldfield, 1978].

For three of the cores (WAP-F, POR-M, and POR-F) sediment chronology was determined using a constant initial concentration (CIC) model [Appleby and Oldfield, 1978]. For WAP-M, ²¹⁰Pb activities varied substantially between samples collected within the depth range of 0–8.5 cm (minimal decay in total ²¹⁰Pb and unsupported ²¹⁰Pb activity) and those collected from deeper intervals (significant decay). Consequently, we chose to use a constant rate of supply (CRS) model [Appleby and Oldfield, 1983] as we expect the mass accumulation rates to vary throughout this surface core chronology.

Eight samples (four plant root samples, two charcoal fragments, one bark fragment, and one shell fragment from the oyster *Saccostrea glomerata*) were selected from among the subsurface sediments of the cores for ¹⁴C dating. The rationale for ¹⁴C dating was primarily to determine the ages of preserved materials, rather

than to infer the ages of sedimentary strata. One root sample did not provide sufficient carbon to progress with the dating. Samples were pretreated to remove any external contaminants. The organic samples underwent acid-alkali-acid treatments to remove possible carbonate and humic acid contaminants, while the shell sample was cleaned by removing the surface with a dental drill, then washed in de-ionized water. Carbon from samples was converted to CO_2 using the sealed-tube method [Hua *et al.*, 2001] then converted to graphite by reduction using excess hydrogen in the presence of an iron catalyst at 600°C for 12 h. Once completed, the graphite and iron mixture was pressed into aluminum cathodes for ^{14}C measurement by accelerator mass spectrometry at Australian Nuclear Science and Technology Organisation (ANSTO) following methods outlined in Fink *et al.* [2004]. The results for the organic samples were calibrated against the SHCal13 calibration curve [Hogg *et al.*, 2013] using OxCal 4.2 [Ramsey, 2009]. A marine reservoir correction was applied to the marine shell sample, as C taken up from marine waters has an older apparent radiocarbon age associated with long C residence times in the deep ocean. This calibration was based upon the global marine calibration curve [Reimer *et al.*, 2013] but also takes into account a regional deviation (ΔR) of 3 ± 69 specific to southeast Australia [Ulm, 2006].

2.7. Elemental and Isotopic Analysis of C and N

In order to calculate and compare C accumulation and C stocks among the four cores, 15 specific depth intervals (10×5 cm depth intervals between 0 and 50 cm; 5×10 cm intervals between 50 and 100 cm) were analyzed for bulk density and %C. Stable isotope ($\delta^{13}\text{C}$) and elemental ratio (C:N) values were also calculated for these depth intervals to assist in identifying the provenance of organic matter. Dried sediment samples were homogenized and ground into a fine powder using a ball mill. The “Champagne test” [Jaschinski *et al.*, 2008] was used to determine if samples contained inorganic C. Only four samples (all from WAP-M core depths >60 cm) contained sufficient carbonate C to cause reaction with HCl. Subsequently, these samples were subject to acid washing with 1 M HCl and shaken for 24 h prior to centrifugation, rinsing with MilliQ water and redrying prior to analysis. Organic %C, %N, and $\delta^{13}\text{C}$ were measured for all samples using an isotope ratio mass spectrometry-elemental analyzer (Thermo DeltaV) at University of Hawaii (HILO). Organic C density (g C cm^{-3}) was determined by multiplying %C/100 by bulk density for each depth interval. Total C stock (Mg C ha^{-1}) was calculated by integrating the 15 depth interval measures over the 0–100 cm depth range.

2.8. ^{13}C NMR

Solid-state ^{13}C NMR (nuclear magnetic resonance) spectroscopy was used to characterize the molecular composition of organic C of all bulk (i.e., inclusive of roots, rhizomes, and sediments) ROI samples [Baldock *et al.*, 2004] and to determine the mechanisms by which organic carbon may have been preserved in marine environments [Dickens *et al.*, 2006]. Briefly, dried, homogenized, and ground sediment samples were treated with 2% hydrofluoric acid [Skjemstad *et al.*, 1994] to remove paramagnetic materials and concentrate C for ^{13}C NMR analyses. Cross-polarization ^{13}C NMR spectra were acquired using a 200 Avance spectrometer (Bruker Corporation, Billerica, MA, USA) following the instrument specifications, experimental procedures, and spectral processing outlined by Baldock *et al.* [2013].

^{13}C NMR spectra (Figure S1 in the supporting information) were used to determine the proportional allocation of C to each of eight spectral regions via integration of acquired signal intensity. The eight regions and the dominant form of carbon represented by each region were as follows: alkylC (0–45 ppm), *N*-alkyl/methoxyl (45–60 ppm), *O*-alkyl (60–95 ppm), Di-*O*-alkyl (95–110 ppm), aryl (110–145 ppm), *O*-aryl (145–165 ppm), amide/carboxyl (165–190 ppm), and ketone (190–215 ppm) [Baldock and Smernik, 2002]. A molecular mixing model described by Nelson and Baldock [2005] was then used to estimate the proportion of key biomolecule components (carbohydrate, protein, lignin, lipid, pure carbonyl, and char) contributing to total C within each ROI. Each of the spectral regions listed above were used as inputs to the molecular mixing model, with amide/carboxyl and ketone combined into a single value (165–215 ppm). The N:C ratio of each ROI was also used to constrain the mixing model [Baldock *et al.*, 2004].

2.9. Grain Size Analysis

Grain size distribution of sediment samples was measured using a laser diffraction particle size analyzer (LS 230; Beckman Coulter, Germany) with an analytical range of 0–2000 μm to estimate the relative energy level present in the environment under which the sediment was transported and deposited [Bartholomä and

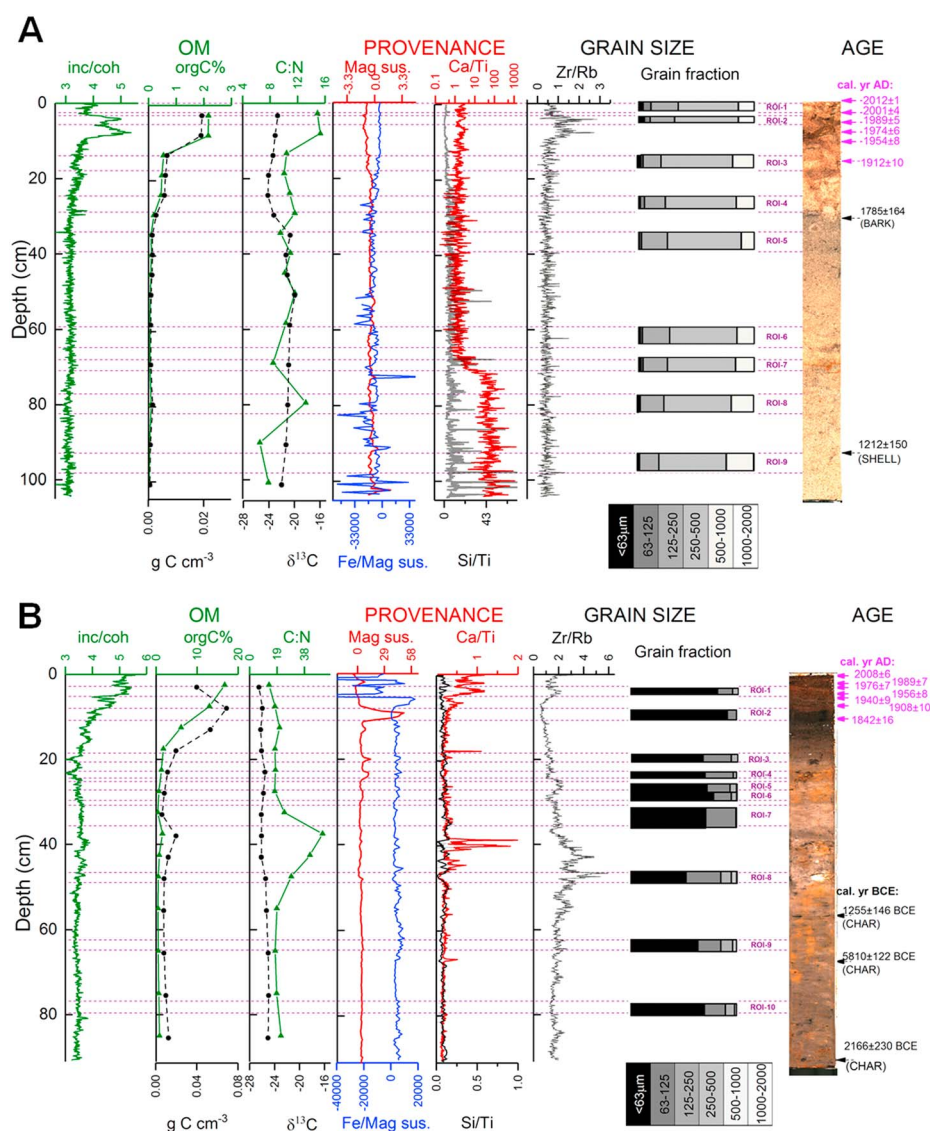


Figure 2. (a) WAP-M and (b) WAP-F core profiles derived from ITRAX core scanning, depth interval, and region of interest (ROI) sampling. Optical core image is presented on the right with ^{210}Pb derived ages presented for surface sediments (pink text) and calibrated ^{14}C ages of specific materials in deeper sections (black text). ROIs for discrete sampling of grain size analysis and molecular composition are labeled and marked by dashed lines.

Flemming, 2007]. Sediments were oxidized with H_2O_2 to remove organic matter and treated with HCl to remove carbonates prior to analysis.

3. Results

3.1. WAP-M

The Wapengo marine core (Figure 2a) displays surface horizons with moderate C densities associated with recent belowground biomass inputs, overlaying OC-poor marine sands, and shells which show little (~ 20 – 30 cm depth) to no (> 30 cm depth) visible record of plant tissue preservation. Radiocarbon dating of deposited materials—tree bark at 30 cm dated to 1785 ± 164 cal years AD and an oyster shell fragment at 91 cm dated to 1212 ± 150 cal years AD (Table 2)—suggests *maximum* long-term surface accretion rates of 1.8 ± 1.8 mm yr^{-1} and 1.2 ± 0.2 mm yr^{-1} , respectively. Recent accumulation rates measured by ^{210}Pb were rapid, relative to the other cores, but were also unique in showing a marked difference in surface accumulation rates in recent (0–8 cm) versus deeper (8–16 cm) sediments (Table 1 and Figure S2).

Table 2. Details of Samples Subjected to Radiocarbon Dating

Site	Lab ID	Depth (cm)	Dated Material	Radiocarbon age ^{14}C year B.P.	1 σ Error	Mean Calibrated Age cal year B.P. ($\pm 2\sigma$)	Mean Calibrated Calendar Age cal year A.D./B.C.E. ($\pm 2\sigma$)
WAP-M	OZT467	29.7–30.7	tree bark	190	30	165 \pm 164	1785 \pm 164 A.D.
	OZT468	90.1–91.2	oyster shell fragment (<i>Saccostrea glomerata</i>)	1180	35	738 \pm 150 ^a	1212 \pm 150 A.D. ^a
WAP-F	OZT469	57.0–58.0	char fragment	3055	35	3205 \pm 146	1255 \pm 146 B.C.E.
	OZT471	58.0–69.0	char fragment	6965	50	7760 \pm 122	5810 \pm 122 B.C.E.
	OZT472	92.0–93.0	char fragment	3790	70	4116 \pm 230	2166 \pm 230 B.C.E.
POR-M	OZT535	54.8–55.9	plant root	1820	30	1688 \pm 108	262 \pm 108 A.D.
	OZT464	86.3–87.4	plant root	1475	35	1331 \pm 52	619 \pm 52 A.D.
POR-F	OZT465	65.3–66.5	plant root	755	40	648 \pm 86	1302 \pm 86 A.D.
	OZT466	108.0–109.2	plant root	Modern			

^aCalibrated using $\Delta R = 3 \pm 69$ years [Ulm, 2006].

Overall, WAP-M had the lowest C stocks of the cores in the present study (Table 1). C density was high in the contemporary root zone (0–10 cm) where C was characterized by high proportions of carbohydrates and lignin (Figure 4). With depth, the proportion of carbohydrate C and carbonyl C declined, most substantially below the contemporary root zone (i.e., ROIs 4 and 5). These declines coincided with increases in the proportions of both proteinaceous and lipid C, while lignin C persisted downcore. Grain size distributions included a greater proportion of <250 μm sediments in contemporary strata (ROIs 1 and 2) but were more coarse and uniform from ROI-3 and below.

3.2. WAP-F

The Wapengo fluvial core (Figure 2b) is characterized by dense organic-rich materials within the surface horizon (0–~15 cm) and multiple depositional facies downcore. Roots were encountered occasionally below the contemporary root zone to the base of the core, but became increasingly sparse with depth. These regions of sparse, fine roots were consistently depleted in $\delta^{13}\text{C}$. A fragment of the volcanic rock pumice was found at 47 cm, while coarse charcoal fragments were present within depositional strata across the entire depth range of the core.

The highest C densities of any core (i.e., 0.04–0.07 g C cm^{-3}) were observed in the surface sediments of WAP-F. Here autochthonous plant contributions (roots, rhizomes, and detritus) were visibly dominant, though ^{13}C NMR analysis showed a substantial contribution (22%) of char in ROI-2. The peak in C density (0.07 g C cm^{-3}) also coincided with three indicators of catchment sedimentation: (1) a significant peak in magnetic susceptibility, (2) low Ca:Ti values, and 3) fine sediment delivery (96% < 63 μm). Below the contemporary root/rhizome zone, C density maintained a baseline of ~0.01 g C cm^{-3} (25–90 cm) with a slight increase associated with a char-rich section between 35 and 40 cm. This baseline C density remained relatively constant despite the decline in the presence of plant roots and rhizomes. Carbohydrates and lignin exhibited substantial decline with depth and were replaced by char, lipids, and to a lesser extent protein and carbonyl C.

3.3. POR-M

The POR-M core shows broad similarity to WAP-M in that both display mineral profiles consistent with a vegetated wetland phase sitting above coarser sediments of apparent marine origin (Figure 3a). In the case of POR-M, however, the fining of sediments was more substantial and extended to a greater depth (~30 cm). Contemporary (up to ~100 year B.P.) bulk sediment and C accumulation rates were also much lower than in WAP-M (Table 1 and Figure S3). Despite this, C stocks over 1 meter of depth were more than four times higher in POR-M relative to WAP-M.

Decays in %C were mirrored by shifts in the character of C from carbohydrate-rich (ROI 1) to carbohydrate poor (ROI 4) strata and a depletion in $\delta^{13}\text{C}$ from -17.6‰ (ROI 1) to -25.5‰ (ROI 4). Below ~25 cm, C density increased to a peak 0.028 g C cm^{-3} and there was a concomitant increase in C:N relative to surface sediments. Visual inspection of the core readily identified partially decayed *Avicennia marina* mangrove roots increasing in density from ~25 cm and persisting to the bottom of the core. In contrast to the shift in C composition observed with depth in the surface sediments, C within the historic mangrove root zone (i.e., ROIs 6–11)

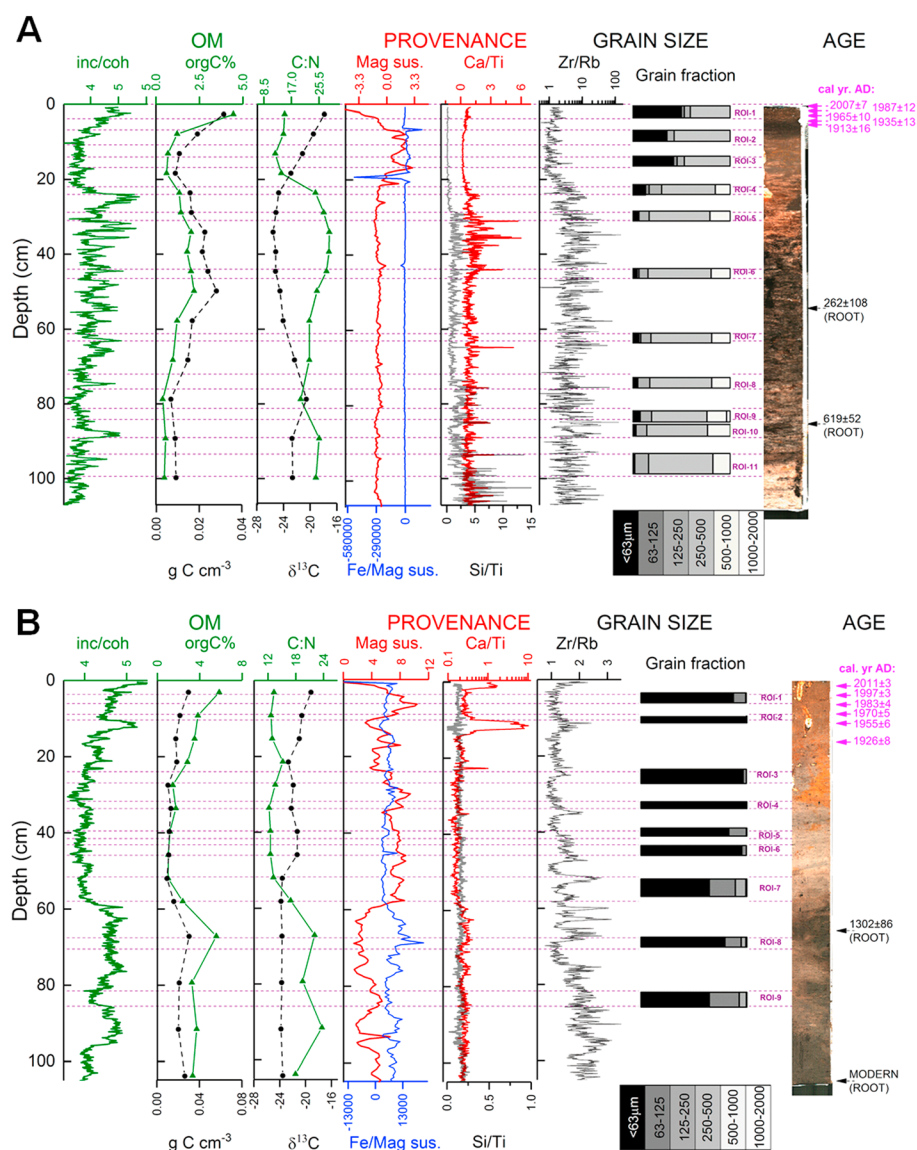


Figure 3. (a) POR-M and (b) POR-F core profiles derived from ITRAX core scanning, depth interval, and region of interest (ROI) sampling. Optical core image is presented on the right with ^{210}Pb derived ages presented for surface sediments (pink text) and calibrated ^{14}C ages of specific materials in deeper sections (black text). ROIs for discrete sampling of grain size analysis and molecular composition are labeled and marked by dashed lines.

appeared stable (Figure 4). That is, plant-derived functional groups dominated, though with the selective retention of lignin relative to carbohydrates. The mineral composition (elevated Ca/Ti and Si/Ti); low magnetic susceptibility and dominance of coarse grains (indicated by both elevated Zr/Rb and discrete measurements of grain size) indicate marine sedimentary inputs below ~ 30 cm.

3.4. POR-F

POR-F contained the highest C stocks over 100 cm of the four cores studied. Surface C accumulation rates were similar to WAP-F, with both higher than those of the marine cores (Table 1 and Figure S3). A large, contemporary mangrove pneumatophore and associated fine roots were observed in the surface sediments (see core image in Figure 3b), coinciding with peaks in inc/coh and $\%C$. Bulk $\delta^{13}\text{C}$ values in the surface 50 cm sat between those of the more enriched roots of the *C4* saltmarsh plant *S. virginicus* (-14.6 to -14.9‰) and the more depleted *A. marina* pneumatophore (-27.4 to -27.9‰) collected from the site, while C:N was mostly constant in the surface 50 cm.

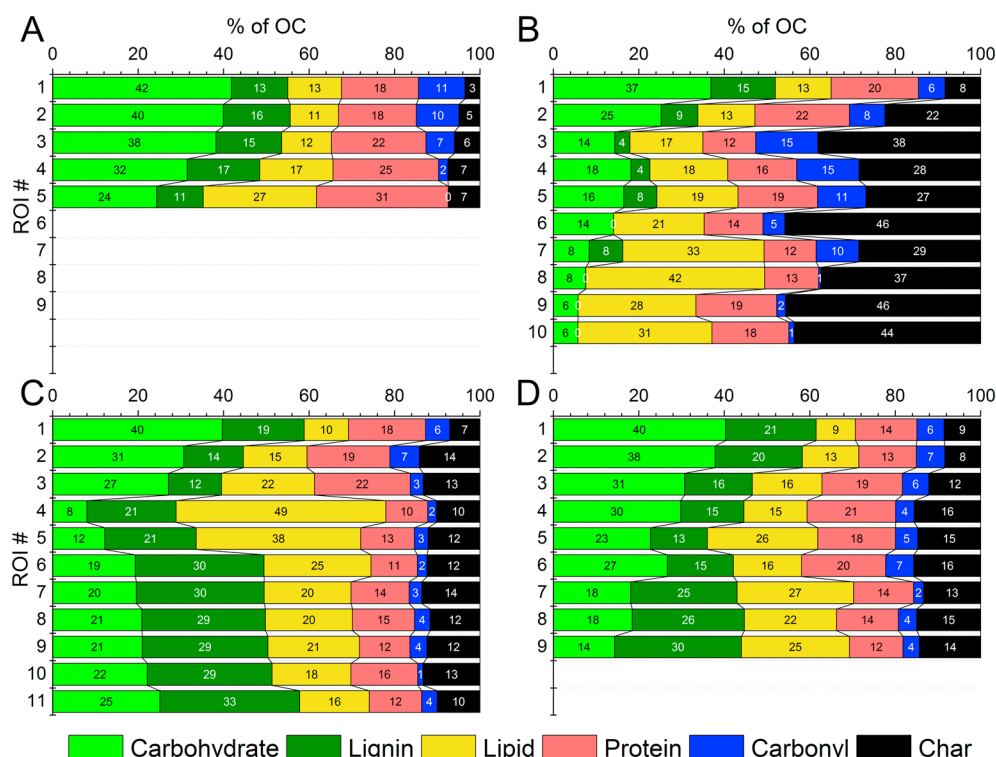


Figure 4. Proportional (%) contributions of six biomolecule groups to organic C in ROIs located throughout the depth range of the four study cores: (a) WAP-M, (b) WAP-F, (c) POR-M, and (d) POR-F. C density was insufficient to obtain reliable ^{13}C NMR spectra for WAP-M ROIs 6–9. For the location of each ROI in each core see corresponding plots in Figures 2 and 3.

Below ~50 cm, sedimentary properties underwent a marked shift, with a broadening of the grain size distribution. Visual inspection of this zone revealed an accumulation of partially decayed *A. marina* mangrove roots, like that seen in POR-M. Radiocarbon analyses of *A. marina* roots at 65 cm and 108 cm returned dates of 1302 ± 86 cal years AD and “modern” (i.e., at or after 1956/7), respectively (Table 2). Like in POR-M, the accumulation of mangrove roots was mirrored by increases in subsurface C:N (Figure 3). While the relative contribution of carbohydrates declined with depth in the POR-F core, there was a marked preservation of plant derived C—mostly lignin—below ROI 6. This decline in carbohydrate C was matched by a relative increase in the contribution of lipids.

4. Discussion

Our detailed analysis of saltmarsh cores revealed different environmental histories and C preservation conditions among the four study sites. Based on the data presented, we interpret the WAP-M core as shifting from a high energy, subtidal elevation (with shell hash at 70 cm and below) to mineral sediments dominated by coarse sands and later to the contemporary (last ~100 years), vegetated saltmarsh surface. The distribution of fine roots only and deposition of strandline materials—e.g., pumice [Ward and Little, 2000] and char—in WAP-F points to a predominantly vegetated, intertidal, to lower supratidal history with no evidence of mangrove or upland tree colonization. At POR-M, the substantial shift in grain size and shift toward terrigenous sediment provenance above ~30 cm is consistent with the capacity of mangrove pneumatophores to slow water movement, and trap fine sediments [Furukawa and Wolanski, 1996]. This sedimentary change, along with the downcore distribution of preserved plant roots, leads us to interpret a historic mangrove colonization (i.e., ~30 cm depth) of previously unvegetated (probably subtidal to lower intertidal) sediments. Although sampled within saltmarsh vegetation, the POR-F core is strongly influenced by both saltmarsh and mangrove belowground biomass, with the latter including both modern and preserved, historic inputs.

4.1. Implications for Blue Carbon Research

Among-site variability has important implications for attempts to characterize blue carbon based on contemporary environmental conditions. Our results suggest that contemporary vegetation structure is likely to be a poor predictor of both C stocks and C accumulation rates. That is, we found approximately threefold, fivefold, and sixfold differences in bulk accumulation, C stock, and C accumulation rates, respectively, among sites characterized by the same vegetation association [Zedler *et al.*, 1995]. For SE Australian saltmarshes this may not be particularly surprising, given that sedimentary factors (rather than vegetation factors) have been identified to be important in predicting saltmarsh C stocks [Kelleway *et al.*, 2016a; Macreadie *et al.*, 2017]. Surface expressions of sediment character and geomorphic setting, however, still fail to account for much of the variability observed in the present study. For example, there are stark differences among the two marine tidal delta cores—WAP-M exhibits faster surface C accumulation, but very low C store, while POR-M exhibits the opposite—slow surface C accumulation, but high C store (Table 1).

The two fluvial cores show some similarity to one another, including above average C stocks relative to regional estimates (regional mean = 164 Mg C ha^{-1}) [Kelleway *et al.*, 2016a] and C accumulation rates for *Sarcocornia-Sporobolus* association saltmarshes ($0.46 \text{ Mg C ha}^{-1} \text{ yr}^{-1}$) [Saintilan *et al.*, 2013]. These similarities occur despite substantial differences in bulk accumulation rates at the two sites (Table 1). That is, the POR-F surface is accumulating bulk materials which are lower in %C, but at a faster rate (2 mm yr^{-1}), which is consistent with accumulation dominated by mineral sediments. In contrast, the exceptionally slow surface accumulation rate and high %C in WAP-F suggest low mineral inputs relative to plant organic matter inputs. Finally, apart from WAP-M, there is also considerable deviation in C stocks from site mean values for each of the cores analyzed in this study (Table 1), despite the expectation of similar geomorphic influences at the within-site scale.

Together, these findings indicate that simple delineations of contemporary vegetation structure and geomorphic setting are not sufficient to explain the spatial variability in blue carbon stocks and accumulation processes. Instead, we need to consider the broader factors of ecosystem stability and environmental change, including historic differences in vegetation and geomorphic processes and the role of C preservation/degradation over time.

4.2. Ecosystem Stability and Environmental Change

Growing interest in blue carbon is based largely upon the potential of saltmarsh, mangrove, and seagrass ecosystems to store C over centennial and millennial time scales. Such a capacity implies an inherent stability within these ecosystems, which is somewhat incongruous with their location within some dynamic areas of estuaries and the coastal ocean [Dalrymple *et al.*, 1992; Roy *et al.*, 2001; Woodroffe *et al.*, 1985]. There are a small number of studies demonstrating exceptional ecosystem stability among seagrass and mangrove ecosystems that were integral to the development of the blue carbon concept. Among these was the discovery of Mediterranean seagrasses which have persisted for over ~5000 years, with continued ecosystem function in the form of C sequestration [Lo Iacono *et al.*, 2008]. That study pointed to stability in local (subtidal) environmental conditions as an important factor in the persistence of seagrass and associated C sequestration. Furthermore, the capacity of intertidal mangrove ecosystems to persist up to 7500 years in the Caribbean, while building belowground C stocks up to 10 m in depth over this time, demonstrates exceptional ecosystem resilience in the face of changing sea level [McKee *et al.*, 2007]. While there are likely to be other instances where either environmental stability or ecosystem resilience leads to ecosystem persistence (and consequently long-term blue carbon accumulation), the results of our study demonstrate that this is not always the case. In fact, our study shows that multiple distinct ecosystem shifts (e.g., unvegetated → mangrove → saltmarsh) may be represented throughout just the surface meter of some blue carbon habitats. This therefore raises important questions—what do ecosystem shifts mean for rates of blue carbon accumulation and storage and what are implications for upscaling blue carbon estimates to broader spatial scales?

4.2.1. Ecosystem Shifts Influence C

Our study shows that ecosystem transitions associated with the geomorphic evolution of estuarine sediments have important implications for C storage. This difference is most evident in the two marine cores where shifts from unvegetated sediments to saltmarsh sediments occurred at both sites. In WAP-M, C inputs appear to be restricted to saltmarsh vegetation which probably only within the past ~100 years. Consequently, this site contains the lowest C stocks (Table 1). Much higher C stocks at POR-M are due in

large part to the occurrence of an intermediate mangrove phase, which persisted for ~300 years or more (Table 2). The downcore expansion of mangrove roots at that time appears to have substantially increased belowground C stocks (Figure 3a). Similarly, the persistence of old and modern mangrove C inputs at POR-F are responsible for much of the overall C stock measured in that core (Figure 3b).

Our records of ecosystem shifts from unvegetated or mangrove-vegetated intertidal to lower supratidal vegetation (saltmarsh) are broadly consistent with the gradual infilling of estuaries proposed by geomorphic models of estuary evolution [Roy, 1984; Roy *et al.*, 2001], whereby fluvial deltas prograde seaward, and (depending on entrance conditions) marine deltas prograde landward. The prograding deltas thereby infill the former mangrove zones with sediments to an extent that their elevation rises in respect to the tidal frame where conditions favor saltmarsh vegetation. Based on evolutionary models, we expect that similar ecosystem shifts would be preserved in similar situations throughout the region.

In this study, mangrove roots were preserved within cores collected from Port Stephens—a drowned river valley in an intermediate evolutionary phase and a broad tidal range. In the nearby Hawkesbury River estuary (also a drowned river estuary in an intermediate state of infilling) *Saintilan and Hashimoto* [1999] found mangrove root systems dating from 500 to 1700 years B.P. preserved ~30 cm below the contemporary saltmarsh surface, highlighting a mangrove to saltmarsh transition associated with the development of the fluvial delta in this location. Similarly, preserved root material at similar depths (from 20 cm below the contemporary surface) also indicated the evolution of sediment surface (relative to local sea level) in the marine settings of Currumbene Creek and Carama Inlet further south in NSW [Saintilan and Wilton, 2001]. At other saltmarsh sites, however, relics of the supratidal tree *Casuarina glauca* within the contemporary saltmarsh [e.g., Kelleway *et al.*, 2016a] indicate a drop in surface elevation relative to local sea level, highlighting the complexity of geomorphic change within estuaries in the same region. Further, while the spatial coverage of blue carbon research has grown throughout the region in recent years, the record of ecosystem shifts below contemporary surface sediments in the region still remains largely unexplored.

Importantly, the preservation of historic blue carbon stocks in settings which have since undergone ecosystem change is not limited to our study region of SE Australia. Across northern Australia, stratigraphic evidence of extensive mangrove root networks below contemporary sedgeland, grasslands, and unvegetated flats was used to demonstrate the occurrence of a “big mangrove swamp” phase in that region between 5500–7000 years B.P. [Woodroffe *et al.*, 1985]. Similarly, extensive coring of Mekong River delta sediments has revealed mangrove, saltmarsh, and tidal flat development below contemporary floodplain and anthropogenic sediments [Hanebuth *et al.*, 2012]. To date, the C storage associated with preserved blue carbon in such locations remains uncalculated, though it may be substantial given the sizes of the deltaic systems involved. Similarly, evidence of successional patterns in mangrove vegetation in locations as diverse as the Mekong delta [Li *et al.*, 2012] to Florida in the southeast USA [Ball, 1980] also remain unquantified in terms of their influence on blue carbon stocks.

4.2.2. Catchment History and Land Use

Environmental changes which do not involve a shift in ecosystem structure may also influence the quantity and quality of C which accumulates in coastal habitats. Recent studies in Australian seagrass beds, for example, have demonstrated shifts in the amount and source of C accumulating in seagrass sediments after post-European settlement modifications to local catchments [Macreadie *et al.*, 2012; Serrano *et al.*, 2016a]. In the present study, evidence of catchment disturbance is most obvious in the WAP-F core where a massive peak in magnetic susceptibility (an indicator of catchment erosion and subsequent deposition) in ROI-2 coincides with the timing of land-clearing for agricultural purposes in the region [NSW National Parks and Wildlife Service, 2011]. Such sedimentation events may play an important role in the preservation of C by shortening oxygen exposure times and creating a reducing environment below which C remineralization efficiency declines [Kristensen, 2000; Kristensen *et al.*, 2008]. More recently, the construction of small farm dams across drainage lines upslope of the saltmarsh has probably created effective sediment traps, starving the wetland of sediments and resulting in extremely slow contemporary surface accumulation relative to other fluvial sites in the region (Table 1) [Rogers *et al.*, 2006].

The role of catchment processes becomes even more distinct in the deeper, pre-European sediments of WAP-F. Here mixing model outputs show char C accounted for almost half of all C in some deep ROIs. The proportion increase in char C in deeper sediments (relative to modern surface sediments) partly reflects

the selective preservation of recalcitrant char with time, highlighting the primary importance of C character to preservation in marine sediments [Dickens *et al.*, 2006]. Variations in char contribution to these deep sediments (shifting from 27% to 46% among adjacent ROIs), however, highlight the temporal variability of char accumulation. Episodic events, including the timing of fires, but also mobilization (e.g., flood) and subsequent deposition (flood and/or tidal deposition) events, dictate the movement of this terrestrial C to blue carbon habitats. It is difficult to determine whether climatic conditions (such as El Niño–Southern Oscillation intensification) or Aboriginal burning practices explain char distribution downcore [Macreadie *et al.*, 2015] though both may play a role. The disparate radiocarbon dates of char fragments in this core profile (Figure 2b and Table 2) suggest that much of this material may be old char which has been redistributed within the catchment. In any case, their ages of 3205 ± 146 , 7760 ± 122 , and 4116 ± 230 calibrated (cal) year B.P., respectively, highlight the long-term preservation potential of this form of C.

Black C typically contributes ~2–30% of the carbon stock of marine sediments [Burdige, 2007], incorporating both char and geological sources [Dickens *et al.*, 2004]. Our char values for many strata within the WAP-F core not only exceeded these marine values but are also high relative to estimates of black C in fire-prone Australian terrestrial soils [Lehmann *et al.*, 2008; Baldock *et al.*, 2013]. Visual inspection of WAP-F clearly showed that fire-derived char was largely responsible for the high C contents measured in that core. Overall, this contribution from char warrants broader research on the contribution of char C to blue carbon stocks, with our preliminary research suggesting that (1) char C contributions may be substantial, (2) is likely to be spatially variable with increased contribution in sites subject to fluvial influence, and (3) is likely to be temporally dependent on catchment processes.

4.3. Preservation of Blue C

In all four cores, declines in C density were matched by shifts in molecular composition in near-surface sediments (Figure 4). This indicates degradation of C that has accumulated during the contemporary saltmarsh phase and is most apparent in the young (~100 year old) saltmarsh at WAP-M. Here C density and C molecular composition display down-core profiles which are broadly consistent with patterns of C decomposition typically seen in terrestrial soils [e.g., Melillo *et al.*, 1989; Rovira and Vallejo, 2002]. Such patterns are contrasted sharply by the preservation of mangrove roots in the POR-M and (to a lesser extent) POR-F cores. The preservation of bulk mangrove roots for at least ~1800 years (POR-M) and ~800 years (POR-F), respectively, suggests a greater C preservation capacity of *A. marina* roots relative to the contemporary *Sarcocornia-Sporobolus* vegetation. This could be due in part to the refractory nature of mangrove roots [Bianchi *et al.*, 2013; McKee *et al.*, 2007; Middleton and McKee, 2001] as evidenced by the selective preservation of lignin C apparent in both cores. However, preservation of some more labile biomolecules (e.g., carbohydrate contents >20% in some deeper ROIs) suggests that other factors associated with deep C preservation may also be important. Principal among these are low microbial activity associated with anaerobic and/or low nutrient conditions [Kristensen *et al.*, 2008; Schmidt *et al.*, 2011].

The effective preservation of mangrove roots has broader implication for blue carbon storage, as mangroves are currently expanding their range globally into saltmarsh ecosystems [Saintilan *et al.*, 2014]. While a recent study has shown that mangrove root development into and above the historic saltmarsh sediment increases total C stocks over a period of 70 years [Kelleway *et al.*, 2016b], the implications for longer-term preservation remain unclear. The findings of enhanced preservation of mangrove root C relative to saltmarsh root and rhizome C in the present study suggest that mangrove encroachment may also lead to longer-term C storage. Clearly though, further research is required here, especially regarding the likely preservation of tissues from a broader range of saltmarsh and mangrove species associated with this global phenomenon of encroachment.

Finally, although appearing less stable than their underlying mangrove roots, the contemporary saltmarsh surface may be playing an important role in the preservation of deeper C stocks. Shallow rooted saltmarsh plants and sediment accumulation associated with the saltmarsh phase appear to effectively cap the below-ground mangrove deposits. This is particularly important where the protrusion of pneumatophores and bioturbation by mangrove fauna may result in increased oxygen diffusion deep into the sediment profile and cause enhanced rates of C remineralization and translocation of CO₂ gas from deeper sediments [Kristensen *et al.*, 2008]. By covering such features, saltmarsh materials effectively remove the historic mangrove C stocks from the oxidizing zone of the surface sediments and confine them to deeper sediments

where microbial remineralization is less efficient. The capacity of saltmarsh vegetation to bind sediments under hydrological phenomena such as sea level rise or tidal forces [Feagin *et al.*, 2009] may also be an important factor in preventing future loss of deeper C stocks.

5. Conclusions

The dynamic nature of estuaries, and specifically their intertidal and lower supratidal zones, means that the environmental history of a site is likely to be a key determinant of current C stocks. Factors including the age of current vegetation communities, the character of preceding vegetation, and biogeochemical conditions may all influence the storage and preservation of organic matter throughout the 0–100 cm depth range (and probably deeper). Specifically, the regional heterogeneity of mangrove root accumulation under contemporary saltmarshes in SE Australia introduces a substantial source of variability when blue carbon stock estimates are upscaled to larger spatial scales based upon contemporary landscape features such as contemporary vegetation maps. In many instances the nature of historic conditions and ecosystem change is difficult to ascertain. Consequently, historical information is largely excluded from regional blue carbon models.

To incorporate the variability introduced by environmental history, researchers and managers will need to find (or generate) information sources which integrate current landscape features with measured or modeled information regarding the geomorphic and vegetation history of locations of interest. In some instances, stratigraphic reconstructions of estuarine or coastal evolution may reveal organic subhorizons indicative of alternate blue carbon habitats. Similarly, acid sulfate soil mapping and modeling [e.g., Smith *et al.*, 2003] may alert users to the distribution of organic-rich subsoils in coastal areas. In some cases, these areas may now support habitats where blue carbon vegetation has been succeeded (e.g., contemporary supratidal floodplains). Where adequate information is not available, targeted sampling and reconstruction of environmental histories may be necessary. Although historically such studies may have been arduous and prohibitively time-consuming, more recent technological advances (such as ITRAX and ^{13}C NMR instruments utilized in this study) may partly ease this cost. Information gained from such studies which reconstruct environmental conditions associated with evolution of blue carbon habitats over past and recent time periods will become increasingly important as coastal wetlands around the world become subject to further anthropogenic, climatic, and sea level-related changes.

Acknowledgments

We thank the many individuals who assisted with field collection, sample preparation, and laboratory analyses, including Frederic Cadera, Janine McGowan, Bruce Hawke, Jack Goralewski, and Fiona Bertuch. Field collections were undertaken in accordance with NSW Office of Environment and Heritage scientific license SL101217 and NSW Department of Primary Industries Scientific Permit P13/0058-1.0. We also thank NSW National Parks and Wildlife Service for supporting access to conservation reserves for fieldwork. This research was supported by the Plant Functional Biology and Climate Change Cluster, CSIRO Coastal Carbon Cluster, and an Australian Institute of Nuclear Science and Engineering AINSE grant (ALNGRA14004) and PGRA grant (ALNSTU11903). We acknowledge the financial support from the Australian Government for the Centre for Accelerator Science at ANSTO through the National Collaborative Research Infrastructure Strategy (NCRIS). P.M. was supported by an Australian Research Council DECRA Fellowship (DE130101084). Data available from the Dryad Digital Repository: <http://dx.doi.org/10.5061/dryad.t6j7f>.

References

- Adam, P., N. Wilson, and B. Huntley (1988), The phytosociology of coastal saltmarsh vegetation in New South Wales, *Wetlands (Australia)*, 7(2), 35–85.
- Adame, M. F., D. Neil, S. F. Wright, and C. E. Lovelock (2010), Sedimentation within and among mangrove forests along a gradient of geomorphological settings, *Estuarine Coastal Shelf Sci.*, 86(1), 21–30.
- Agnihotri, R., M. A. Altabet, T. D. Herbert, and J. E. Tierney (2008), Subdecadally resolved paleoceanography of the Peru margin during the last two millennia, *Geochim. Geophys. Geosyst.*, 9, Q05013, doi:10.1029/2007GC001744.
- Alongi, D. M. (2002), Present state and future of the world's mangrove forests, *Environ. Conserv.*, 29(3), 331–349.
- Appleby, P., and F. Oldfield (1978), The calculation of lead-210 dates assuming a constant rate of supply of unsupported ^{210}Pb to the sediment, *Catena*, 5(1), 1–8.
- Appleby, P., and F. Oldfield (1983), The assessment of ^{210}Pb data from sites with varying sediment accumulation rates, *Hydrobiologia*, 103, 29–35, doi:10.1007/BF00028424.
- Atahan, P., H. Heijnis, J. Dodson, K. Grice, P. Le Métayer, K. Taffs, S. Hembrow, M. Wolterring, and A. Zawadzki (2015), Pollen, biomarker and stable isotope evidence of late Quaternary environmental change at Lake McKenzie, southeast Queensland, *J. Paleolimnol.*, 53(1), 139–156.
- Baldock, J. A., and R. J. Smernik (2002), Chemical composition and bioavailability of thermally altered *Pinus resinosa* (red pine) wood, *Org. Geochem.*, 33(9), 1093–1109, doi:10.1016/S0146-6380(02)00062-1.
- Baldock, J. A., C. Masiello, Y. Gelinas, and J. Hedges (2004), Cycling and composition of organic matter in terrestrial and marine ecosystems, *Mar. Chem.*, 92(1), 39–64.
- Baldock, J. A., J. Sanderman, L. M. Macdonald, A. Puccini, B. Hawke, S. Szarvas, and J. McGowan (2013), Quantifying the allocation of soil organic carbon to biologically significant fractions, *Soil Res.*, 51(8), 561, doi:10.1071/sr12374.
- Ball, M. C. (1980), Patterns of secondary succession in a mangrove forest of southern Florida, *Oecologia*, 44(2), 226–235.
- Bartholomä, A., and B. W. Flemming (2007), Progressive grain-size sorting along an intertidal energy gradient, *Sediment. Geol.*, 202(3), 464–472, doi:10.1016/j.sedgeo.2007.03.010.
- Bianchi, T. S., M. A. Allison, J. Zhao, X. Li, R. S. Comeaux, R. A. Feagin, and R. W. Kulawardhana (2013), Historical reconstruction of mangrove expansion in the Gulf of Mexico: Linking climate change with carbon sequestration in coastal wetlands, *Estuarine Coastal Shelf Sci.*, 119, 7–16.
- Burdige, D. J. (2007), Preservation of organic matter in marine sediments: Controls, mechanisms, and an imbalance in sediment organic carbon budgets?, *Chem. Rev.*, 107(2), 467–485.

- Burnett, A. P., M. J. Soreghan, C. A. Scholz, and E. T. Brown (2011), Tropical East African climate change and its relation to global climate: A record from Lake Tanganyika, tropical East Africa, over the past 90+ kyr, *Palaeogeogr. Palaeoclimatol. Palaeoecol.*, **303**(1–4), 155–167, doi:10.1016/j.palaeo.2010.02.011.
- Chen, Y., G. Chen, and Y. Ye (2015), Coastal vegetation invasion increases greenhouse gas emission from wetland soils but also increases soil carbon accumulation, *Sci. Total Environ.*, **526**, 19–28.
- Clarke, P. J., and C. A. Jacoby (1994), Biomass and above-ground productivity of salt-marsh plants in south-eastern Australia, *Mar. Freshwater Res.*, **45**(8), 1521–1528.
- Creese, R., T. Glasby, G. West, and C. Gallen (2009), Mapping the habitats of NSW estuaries, Rep., 95 pp., Industry & Investment NSW, Port Stephens, NSW, Australia.
- Croudace, I. W., A. Rindby, and R. G. Rothwell (2006), ITRAX: Description and evaluation of a new multi-function X-ray core scanner, *Geol. Soc. London Spec. Publ.*, **267**, 51.
- Dalrymple, R. W., B. A. Zaitlin, and R. Boyd (1992), Estuarine facies models: Conceptual basis and stratigraphic implications: Perspective, *J. Sediment. Res.*, **62**(6).
- Davies, G. (2011), Downstream changes in the cross-sectional shape of tidal channels.
- Derenne, S., and C. Largeau (2001), A review of some important families of refractory macromolecules: Composition, origin, and fate in soils and sediments, *Soil Sci.*, **166**(11), 833–847.
- Dickens, A. F., J. A. Baldock, R. J. Smernik, S. G. Wakeham, T. S. Arnarson, Y. Gélinas, and J. I. Hedges (2006), Solid-state ^{13}C NMR analysis of size and density fractions of marine sediments: Insight into organic carbon sources and preservation mechanisms, *Geochim. Cosmochim. Acta*, **70**(3), 666–686, doi:10.1016/j.gca.2005.10.024.
- Dickens, A. F., Y. Gélinas, C. A. Masiello, S. Wakeham, and J. I. Hedges (2004), Reburial of fossil organic carbon in marine sediments, *Nature*, **427**(6972), 336–339.
- Donato, D. C., J. B. Kauffman, D. Murdiyarso, S. Kurnianto, M. Stidham, and M. Kanninen (2011), Mangroves among the most carbon-rich forests in the tropics, *Nat. Geosci.*, **4**(5), 293–297.
- Duarte, C. M., I. J. Losada, I. E. Hendriks, I. Mazarrasa, and N. Marbà (2013), The role of coastal plant communities for climate change mitigation and adaptation, *Nat. Clim. Change*, **3**(11), 961–968.
- Enríquez, S., C. M. Duarte, and K. Sand-Jensen (1993), Patterns in decomposition rates among photosynthetic organisms: The importance of detritus C:N:P content, *Oecologia*, **94**(4), 457–471.
- Feagin, R., S. Lozada-Bernard, T. Ravens, I. Möller, K. Yeager, and A. Baird (2009), Does vegetation prevent wave erosion of salt marsh edges?, *Proc. Natl. Acad. Sci. U.S.A.*, **106**(25), 10,109–10,113.
- Fink, D., M. Hotchkis, Q. Hua, G. Jacobsen, A. Smith, U. Zoppi, D. Child, C. Mifsud, H. van der Gaast, and A. Williams (2004), The Antares AMS facility at ANSTO, *Nucl. Instrum. Methods Phys. Res., Sect. B*, **223**, 109–115.
- Fourqurean, J. W., C. M. Duarte, H. Kennedy, N. Marbà, M. Holmer, M. A. Mateo, E. T. Apostolaki, G. A. Kendrick, D. Krause-Jensen, and K. J. McGlathery (2012), Seagrass ecosystems as a globally significant carbon stock, *Nat. Geosci.*, **5**(7), 505–509.
- Furukawa, K., and E. Wolanski (1996), Sedimentation in mangrove forests, *Mangrove Salt Marshes*, **1**(1), 3–10.
- Grandy, A. S., and J. C. Neff (2008), Molecular C dynamics downstream: The biochemical decomposition sequence and its impact on soil organic matter structure and function, *Sci. Total Environ.*, **404**(2–3), 297–307, doi:10.1016/j.scitotenv.2007.11.013.
- Hanebuth, T. J. J., U. Proske, Y. Saito, V. L. Nguyen, and T. K. O. Ta (2012), Early growth stage of a large delta—Transformation from estuarine-platform to deltaic-progradational conditions (the northeastern Mekong River Delta, Vietnam), *Sediment. Geol.*, **261**–262, 108–119, doi:10.1016/j.sedgeo.2012.03.014.
- Hofmann, D. I., K. Fabian, F. Schmieder, B. Donner, and U. Bleil (2005), A stratigraphic network across the subtropical front in the central South Atlantic: Multi-parameter correlation of magnetic susceptibility, density, X-ray fluorescence and $\delta^{18}\text{O}$ records, *Earth Planet. Sci. Lett.*, **240**(3), 694–709.
- Hogg, A., Q. Hua, P. Blackwell, M. Niu, C. Buck, T. Guilderson, T. Heaton, J. Palmer, P. Reimer, and R. Reimer (2013), SHCal13 southern hemisphere calibration, 0–50,000 cal yr BP, *Radiocarbon*, **55**, 1889–1903.
- Howes, B. L., J. W. Dacey, and G. M. King (1984), Carbon flow through oxygen and sulfate reduction pathways in salt marsh sediments, *Limnol. Oceanogr.*, **29**, 1037–1051.
- Hua, Q., G. Jacobsen, U. Zoppi, E. Lawson, A. Williams, A. Smith, and M. McGann (2001), Progress in radiocarbon target preparation at the ANTARES AMS Centre, *Radiocarbon*, **43**(2; PART A), 275–282.
- Jaschinski, S., T. Hansen, and U. Sommer (2008), Effects of acidification in multiple stable isotope analyses, *Limnol. Oceanogr. Methods*, **6**(1), 12–15, doi:10.4319/lom.2008.6.12.
- Kelleway, J. J., N. Saintilan, P. I. Macreadie, and P. J. Ralph (2016a), Sedimentary factors are key predictors of carbon storage in SE Australian saltmarshes, *Ecosystems*, doi:10.1007/s10021-016-9972-3.
- Kelleway, J. J., N. Saintilan, P. I. Macreadie, C. G. Skilbeck, A. Zawadzki, and P. J. Ralph (2016b), Seventy years of continuous encroachment substantially increases ‘blue carbon’ capacity as mangroves replace intertidal salt marshes, *Global Change Biol.*, **22**, 1097–1109, doi:10.1111/gcb.13158.
- Kennedy, H., J. Beggins, C. M. Duarte, J. W. Fourqurean, M. Holmer, N. Marbà, and J. J. Middelburg (2010), Seagrass sediments as a global carbon sink: Isotopic constraints, *Global Biogeochem. Cycles*, **24**, GB4026, doi:10.1029/2010GB003848.
- King, G. M. (1983), Sulfate reduction in Georgia salt marsh soils: An evaluation of pyrite formation by use of ^{35}S and ^{55}Fe tracers, *Limnol. Oceanogr.*, **28**, 987–995.
- Kirwan, M. L., J. A. Langley, G. R. Guntenspergen, and J. P. Megonigal (2013), The impact of sea-level rise on organic matter decay rates in Chesapeake Bay brackish tidal marshes, *Biogeosciences*, **10**(3), 1869–1876, doi:10.5194/bg-10-1869-2013.
- Kirwan, M. L., and J. P. Megonigal (2013), Tidal wetland stability in the face of human impacts and sea-level rise, *Nature*, **504**(7478), 53–60, doi:10.1038/nature12856.
- Kristensen, E. (1994), Decomposition of macroalgae, vascular plants and sediment detritus in seawater: Use of stepwise thermogravimetry, *Biogeochemistry*, **26**(1), 1.
- Kristensen, E. (2000), Organic matter diagenesis at the oxic/anoxic interface in coastal marine sediments, with emphasis on the role of burrowing animals, *Hydrobiologia*, **426**(1), 1–24.
- Kristensen, E., S. Bouillon, T. Dittmar, and C. Marchand (2008), Organic carbon dynamics in mangrove ecosystems: A review, *Aquat. Bot.*, **89**(2), 201–219.
- Lehmann, J., J. Skjemstad, S. Sohi, J. Carter, M. Barson, P. Falloon, K. Coleman, P. Woodbury, and E. Krull (2008), Australian climate–carbon cycle feedback reduced by soil black carbon, *Nat. Geosci.*, **1**(12), 832–835, doi:10.1038/ngeo358.

- Li, Z., Y. Saito, L. Mao, T. Tamura, Z. Li, B. Song, Y. Zhang, A. Lu, S. Sieng, and J. Li (2012), Mid-Holocene mangrove succession and its response to sea-level change in the upper Mekong River delta, Cambodia, *Quat. Res.*, 78(2), 386–399, doi:10.1016/j.yqres.2012.07.001.
- Lo Iacono, C., M. A. Mateo, E. Gràcia, L. Guasch, R. Carbonell, L. Serrano, O. Serrano, and J. Dañoibeitia (2008), Very high-resolution seismo-acoustic imaging of seagrass meadows (Mediterranean Sea): Implications for carbon sink estimates, *Geophys. Res. Lett.*, 35, L18601, doi:10.1029/2008GL034773.
- Lord III, C. J., and T. M. Church (1983), The geochemistry of salt marshes: Sedimentary ion diffusion, sulfate reduction, and pyritization, *Geochim. Cosmochim. Acta*, 47(8), 1381–1391, doi:10.1016/0016-7037(83)90296-X.
- Lovelock, C. E., M. F. Adame, V. Bennion, M. Hayes, J. O'Mara, R. Reef, and N. S. Santini (2013), Contemporary rates of carbon sequestration through vertical accretion of sediments in mangrove forests and saltmarshes of south East Queensland, Australia, *Estuaries Coasts*, 37(3), 763–771, doi:10.1007/s12237-013-9702-4.
- Macreadie, P. I., K. Allen, B. P. Kelaher, P. J. Ralph, and C. G. Skilbeck (2012), Paleoreconstruction of estuarine sediments reveal human-induced weakening of coastal carbon sinks, *Global Change Biol.*, 18(3), 891–901, doi:10.1111/j.1365-2486.2011.02582.x.
- Macreadie, P. I., T. C. Rolph, R. Boyd, C. J. Schroder-Adams, and C. G. Skilbeck (2015), Do ENSO and coastal development enhance coastal burial of terrestrial carbon?, *PLoS One*, 10(12), e0145136, doi:10.1371/journal.pone.0145136.
- Macreadie, P. I., et al. (2017), Carbon sequestration by Australian tidal marshes, *Sci. Rep.*, 7, 44071, doi:10.1038/srep44071.
- McKee, K. L., D. R. Cahoon, and I. C. Feller (2007), Caribbean mangroves adjust to rising sea level through biotic controls on change in soil elevation, *Global Ecol. Biogeogr.*, 16(5), 545–556.
- McLeod, E., G. L. Chmura, S. Bouillon, R. Salm, M. Björk, C. M. Duarte, C. E. Lovelock, W. H. Schlesinger, and B. R. Silliman (2011), A blueprint for blue carbon: Toward an improved understanding of the role of vegetated coastal habitats in sequestering CO₂, *Front. Ecol. Environ.*, 9(10), 552–560, doi:10.1890/110004.
- Melillo, J. M., J. D. Aber, A. E. Linkins, A. Ricca, B. Fry, and K. J. Nadelhoffer (1989), Carbon and nitrogen dynamics along the decay continuum: Plant litter to soil organic matter, in *Ecology of Arable Land—Perspectives and Challenges*, pp. 53–62, Springer, Dordrecht, Holland.
- Middleton, B. A., and K. L. McKee (2001), Degradation of mangrove tissues and implications for peat formation in Belizean island forests, *J. Ecol.*, 89(5), 818–828, doi:10.1046/j.0022-0477.2001.00602.x.
- Mitchell, M., and P. Adam (1989), The relationship between mangrove and saltmarsh communities in the Sydney region, *Wetlands (Australia)*, 8(2), pp. 37–46.
- Nelson, P. N., and J. A. Baldock (2005), Estimating the molecular composition of a diverse range of natural organic materials from solid-state ¹³C NMR and elemental analyses, *Biogeochemistry*, 72(1), 1–34, doi:10.1007/s10533-004-0076-3.
- Nixon, S. W. (1980), Between coastal marshes and coastal waters: A review of twenty years of speculation and research on the role of salt marshes in estuarine productivity and water chemistry, URI, Marine Advisory Service, Publications Unit.
- NSW National Parks and Wildlife Service (2011), Mimosas Rocks National Park Plan of Management, Rep. 978 1 74293 219 4, 86 pp., Dep. of Environ., Clim. Change and Water.
- Pendleton, L., D. C. Donato, B. C. Murray, S. Crooks, W. A. Jenkins, S. Sifleet, C. Craft, J. W. Fourqurean, J. B. Kauffman, and N. Marbà (2012), Estimating global “blue carbon” emissions from conversion and degradation of vegetated coastal ecosystems, *PLoS One*, 7(9), e43542.
- Ramsey, C. B. (2009), Bayesian analysis of radiocarbon dates, *Radiocarbon*, 51(1), 337–360.
- Reimer, P. J., E. Bard, A. Bayliss, J. W. Beck, P. G. Blackwell, C. B. Ramsey, C. E. Buck, H. Cheng, R. L. Edwards, and M. Friedrich (2013), IntCal13 and Marine13 radiocarbon age calibration curves 0–50,000 years cal BP, *Radiocarbon*, 55(4), 1869–1887.
- Ricart, A. M., P. H. York, M. A. Rasheed, M. Pérez, J. Romero, C. V. Bryant, and P. I. Macreadie (2015), Variability of sedimentary organic carbon in patchy seagrass landscapes, *Mar. Pollut. Bull.*, 100(1), 476–482.
- Rogers, K., K. M. Wilton, and N. Saintilan (2006), Vegetation change and surface elevation dynamics in estuarine wetlands of southeast Australia, *Estuarine Coastal Shelf Sci.*, 66(3–4), 559–569, doi:10.1016/j.ecss.2005.11.004.
- Roper, T., B. Creese, P. Scanes, K. Stephens, R. Williams, J. Dela-Cruz, G. Coade, B. Coates, and M. Fraser (2011), Assessing the condition of estuaries and coastal lake ecosystems in NSW, *NSW State Catchments 2010*, 239.
- Rothwell, R. G., and I. W. Croudace (2015), Twenty years of XRF core scanning marine sediments: What do geochemical proxies tell us?, in *Micro-XRF Studies of Sediment Cores*, pp. 25–102, Springer, Dordrecht, Holland.
- Rovira, P., and V. R. Vallejo (2002), Labile and recalcitrant pools of carbon and nitrogen in organic matter decomposing at different depths in soil: An acid hydrolysis approach, *Geoderma*, 107(1–2), 109–141, doi:10.1016/S0016-7061(01)00143-4.
- Roy, P. (1984), New South Wales Estuaries: Their Origin and Evolution, in *Coastal Geomorphology in Australia*, edited by B. G. Thom, pp., 99–121, Academic Press, Sydney.
- Roy, P., and R. Boyd (1996), Quaternary geology of southeast Australia: A tectonically stable, wave-dominated, sediment deficient margin, Field Guide to the Central New South Wales Coast, IGCP Project# 367, paper presented at International Conference, Sydney.
- Roy, P., and L. Matthei (1996), Late Cainozoic clay deposits in the Port Stephens area, New South Wales, *Aust. J. Earth Sci.*, 43(4), 395–400.
- Roy, P., R. Williams, A. Jones, I. Yassini, P. Gibbs, B. Coates, R. West, P. Scanes, J. Hudson, and S. Nichol (2001), Structure and function of south-east Australian estuaries, *Estuarine Coastal Shelf Sci.*, 53(3), 351–384.
- Roy, P. S., and B. G. Thom (1981), Late Quaternary marine deposition in New South Wales and southern Queensland—An evolutionary model, *J. Geol. Soc. Aust.*, 28(3–4), 471–489, doi:10.1080/00167618108729182.
- Saintilan, N., and T. Hashimoto (1999), Mangrove-saltmarsh dynamics on a bay-head delta in the Hawkesbury River estuary, New South Wales, Australia, *Hydrobiologia*, 413, 95–102.
- Saintilan, N., and K. Wilton (2001), Changes in the distribution of mangroves and saltmarshes in Jervis Bay, Australia, *Wetl. Ecol. Manage.*, 9(5), 409–420.
- Saintilan, N., K. Rogers, D. Mazumder, and C. Woodroffe (2013), Allochthonous and autochthonous contributions to carbon accumulation and carbon store in southeastern Australian coastal wetlands, *Estuarine Coastal Shelf Sci.*, 128, 84–92.
- Saintilan, N., N. C. Wilson, K. Rogers, A. Rajkaran, and K. W. Krauss (2014), Mangrove expansion and salt marsh decline at mangrove poleward limits, *Global Change Biol.*, 20(1), 147–157, doi:10.1111/gcb.12341.
- Schmidt, M. W., et al. (2011), Persistence of soil organic matter as an ecosystem property, *Nature*, 478(7367), 49–56, doi:10.1038/nature10386.
- Serrano, O., P. Lavery, P. Masque, K. Inostroza, J. Bongiovanni, and C. Duarte (2016a), Seagrass sediments reveal the long-term deterioration of an estuarine ecosystem, *Global Change Biol.*, doi:10.1111/gcb.13195.
- Serrano, O., P. S. Lavery, C. M. Duarte, G. A. Kendrick, P. York, A. Steven, and P. Macreadie (2016b), Can mud (silt and clay) concentration be used to predict soil organic carbon content within seagrass ecosystems?, *Biogeosci. Discuss.*, 2016, 1–24, doi:10.5194/bg-2015-598.

- Skjemstad, J., P. Clarke, J. Taylor, J. Oades, and R. Newman (1994), The removal of magnetic materials from surface soils—a solid state ^{13}C CP/MAS NMR study, *Soil Res.*, 32(6), 1215–1229.
- Smith, J., P. van Oploo, H. Marston, M. D. Melville, and B. C. T. Macdonald (2003), Spatial distribution and management of total actual acidity in an acid sulfate soil environment, McLeods Creek, northeastern NSW, Australia, *Catena*, 51(1), 61–79, doi:10.1016/S0341-8162(02)00069-3.
- Swales, A., S. J. Bentley, and C. E. Lovelock (2015), Mangrove-forest evolution in a sediment-rich estuarine system: Opportunists or agents of geomorphic change?, *Earth Surf. Processes Landforms*, 40(12), 1672–1687, doi:10.1002/esp.3759.
- Trevathan-Tackett, S. M., J. J. Kelleway, P. I. Macreadie, J. Beardall, P. Ralph, and A. Bellgrove (2015), Comparison of marine macrophytes for their contributions to blue carbon sequestration, *Ecology*, 96(11), 3043–3057.
- Ulm, S. (2006), Australian marine reservoir effects: A guide to ΔR values, *Aust. Archaeol.*, 63, 57–60.
- van der Land, C., F. Mienis, H. de Haas, H. C. de Stigter, R. Swennen, J. J. G. Reijmer, and T. C. E. van Weering (2011), Paleo-redox fronts and their formation in carbonate mound sediments from the Rockall Trough, *Mar. Geol.*, 284(1–4), 86–95, doi:10.1016/j.margeo.2011.03.010.
- Ward, W., and I. Little (2000), Sea-rafted pumice on the Australian east coast: Numerical classification and stratigraphy, *Aust. J. Earth Sci.*, 47(1), 95–109.
- West, R. J., C. Thorogood, T. Walford, and R. Williams (1985), *An Estuarine Inventory for New South Wales, Australia*, pp. 1–140, Fisheries Bulletin, Department of Agriculture New South Wales, Sydney, Australia.
- Woodroffe, C. D., B. G. Thom, and J. Chappell (1985), Development of widespread mangrove swamps in mid-Holocene times in northern Australia, *Nature*, 317(6039), 711–713.
- Zedler, J., P. Nelson, and P. Adam (1995), Plant community organization in New South Wales saltmarshes: Species mosaics and potential causes, *Wetlands (Australia)*, 14(1), 1–18.
- Zhou, J., Y. Wu, J. Zhang, Q. Kang, and Z. Liu (2006), Carbon and nitrogen composition and stable isotope as potential indicators of source and fate of organic matter in the salt marsh of the Changjiang estuary, China, *Chemosphere*, 65(2), 310–317, doi:10.1016/j.chemosphere.2006.02.026.